EPSC Abstracts
Vol. 13, EPSC-DPS2019-61-3, 2019
EPSC-DPS Joint Meeting 2019

EPSC
EPSC-DPS Joint Meeting 2019
15–20 September 2019 | Geneva, Switzerland

Evidence for Impact Induced Liberation of Solar Wind Generated Volatiles

Jeffrey J. Gillis-Davis (1), Josiah B. Lewis (2), Ryan C. Ogliore (2) Hope A. Ishii (1), John P. Bradley (1) Ralf I. Kaiser (3), Cheng Zhu (3).

(1) University of Hawai'i at Mānoa, Hawai'i Institute of Geophysics and Planetology, Honolulu, Hawaii, 96822, USA, (2) Laboratory for Space Sciences, and Department of Physics, Washington University, St. Louis, Missouri, 63130, USA (3) University of Hawai'i at Mānoa, Department of Chemistry, Honolulu, HI 96822. USA (1) gillis@higp.hawaii.edu

Abstract

Electron microscopy of two lunar impact melts reveals evidence for the formation of H_2O/OH on the Moon and other airless bodies by a two-step process: solar wind implantation and micrometeorite impact.

1. Introduction

The lunar water cycle is a complex system with multiple sources. Contributing water sources are: primordial water expelled from the interior of the Moon by geologic processes [5,6], solar wind produced water [4,8], and impact generated water [1,7]. Impactors either are hydrous and release their water upon impact [1,7] or release ancient water trapped beneath a desiccated soil layer [2]. Determining the relative contribution of each of these three sources to the exosphere and polar ice deposits is a key factor to understanding the lunar water cycle.

Here we report on a synergistic source for the formation and liberation of water that requires solar wind implantation and micrometeorite impacts. This model was developed based on dual ion and laser irradiation experiments [9] and transmission electron microscopy (TEM) of interplanetary dust particles [3]. Evidence for micrometeorite impact induced liberation of volatiles is observed in samples from experiments, lunar soils, and meteorite regoliths.

2. Methods

Grains from a mature Apollo 11 soil 10084 were mounted and carbon-coated for scanning electron microscopy (SEM) and future Focused Ion Beam (FIB) milling and atom probe analyses. Surfaces of individual grains were imaged with secondary electron imaging using Washington University's FEI

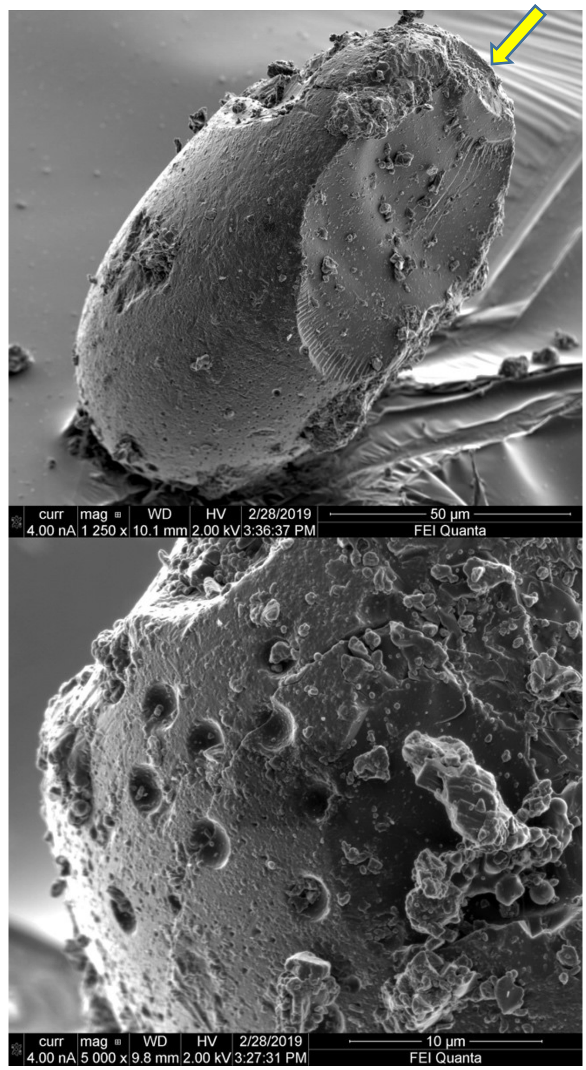

Figure 1a: (Top) A Secondary electron image of an impact melt glass ellipsoid, standing at a ~45° angle to the mount, with a zap pit at its upper end (arrow). 1b (bottom) is a high-resolution image that reveals small pits (~2 µm) along the rim of the impact crater.

3D FEG Dual Beam FIB. Surfaces were examined for burst vesicles and zap pits (i.e., micrometeorite impact craters). These surface pits will be selected for electron-transparent thin section preparation using the FEI Helios 660 dual beam FIB at the University of Hawaii. TEM imaging of FIB cross-sections will be done with FEI high-base Titan G2 60-300 keV monochromated and dual aberration-corrected (scanning) TEM. Imaging will be used to characterize textures and nanoparticles of iron metal, elemental chemical mapping will be done by energy dispersive X-ray spectroscopy, and Valence Electron Energy Loss spectra will be collected for detection of hydroxyl/water features.

3. Results

Two ellipsoidal impact melt glasses were examined. The shape results from tumbling during ballistic flight, and the glassy property indicates quenching. The first grain is 110×225 µm in size, and the second glass grain is 60×100 µm. The first/larger grain has a smooth pit-free surface. The smaller of the two grains has a zap pit, ~20 µm in diameter, at the tip of one of the long ends of the ellipsoid (Fig 1a). One half of the glass bead has broken off to reveal the crater in cross section. Fracture striations radiate beneath the central portion of the crater and where the cleaved surface intersects the bead's original surface. Two populations of pits, similar to those seen in [9], are found approximately antipodal to the impact crater and along the portion of the crater rim that still exists (Fig 1b). The pits on this grain occur in a bimodal size distribution: the smaller pits average size is ~0.5 µm, while the larger pits average size is ~2 µm. Five to eight of larger pits are found in a ~200 μm^2 area. The smaller pits are more prevalent (10:1) than the larger pits. The larger pits are also more circular and exhibit blistering from solar wind implantation.

4. Summary and Conclusions

The two glass grains have presumed similar solar wind exposure. 1 keV solar wind hydrogen bonds with metal ions within the glass. We propose the following formation for the observed features. In the grain that lacks the zap pit, hydrogen was not released by diurnal heating. In the grain with the zap pit, the thermal shock released implanted hydrogen in the form of water/hydroxyl. The H_2O/OH gas formed vesicles and the resulting overpressure created the pits. The morphology of these two grains presents compelling evidence of the efficient formation and liberation of H_2O/OH from anhydrous melt glass upon solar wind ion irradiation and subsequent impact. Observational evidence of the associated solar wind–micrometeorite impact induced formation of water, suggests that lunar water production cannot be attributed solely to either a solar wind source or micrometeorite impacts. This synergistic water production model would have far-reaching effects beyond the Moon because similar processes occur on all airless bodies in our Solar System.

Acknowledgements

This work was funded by NASA SSW grant NNX16AR80G to JJGD and Ogliore startup funds to support a portion of Lewis' time.

References

[1] Arnold, J., 1979. Ice in the lunar polar regions. J. Geophys. Res. 84, 5659-5668.

[2] Benna, M., Hurley, D. M., Stubbs, T. J., Mahaffy, P. R., Elphic, R. C., 2019. Lunar soil hydration constrained by exospheric water liberated by meteoroid impacts. Nature Geoscience.

[3] Bradley, J. P., et al., 2014. Detection of solar wind-produced water in irradiated rims on silicate minerals. PNAS. 111**,** 1732-1735.

[4] Hurley, D. M., et al., 2017. Contributions of solar wind and micrometeoroids to molecular hydrogen in the lunar exosphere. Icarus. 283, 31-37.

[5] Needham, D. H., Kring, D. A., 2017. Lunar volcanism produced a transient atmosphere around the ancient Moon. Earth and Planetary Science Letters. 478, 175-178.

[6] Saal, A.E., Hauri, E.H., Cascio, M.L., Van Orman, J.A., Rutherford, M.C., & Cooper, R.F., 2008. Volatile content of lunar volcanic glasses and the presence of water in the Moon's interior. Nature 454 (7201):192.

[7] Watson, K., Murray, B. C., Brown, H., 1961. The behavior of volatiles on the lunar surface. J. Geophys. Res. 66, 3033-3045.

[8] Zeller E, Ronca LB, & Levy P., 1966. Proton ‐ induced hydroxyl formation on the lunar surface. J Geophys Res 71(20):4855-4860.

[9] Zhu, C., et al., 2019. Untangling the formation and liberation of water in the lunar regolith. Proceedings of the National Academy of Sciences. *Accepted*.